Cell Stem Cell, Volume *7*

Supplemental Information

mTOR Activation Induces Tumor Suppressors that Inhibit Leukemogenesis and Deplete Hematopoietic Stem Cells after *Pten* Deletion

Jae Y. Lee, Daisuke Nakada, Omer H. Yilmaz, Zuzana Tothova, Nancy M. Joseph, Megan S. Lim, D. Gary Gilliland, and Sean J. Morrison

INVENTORY OF THE SUPPLEMENTARY INFORMATION

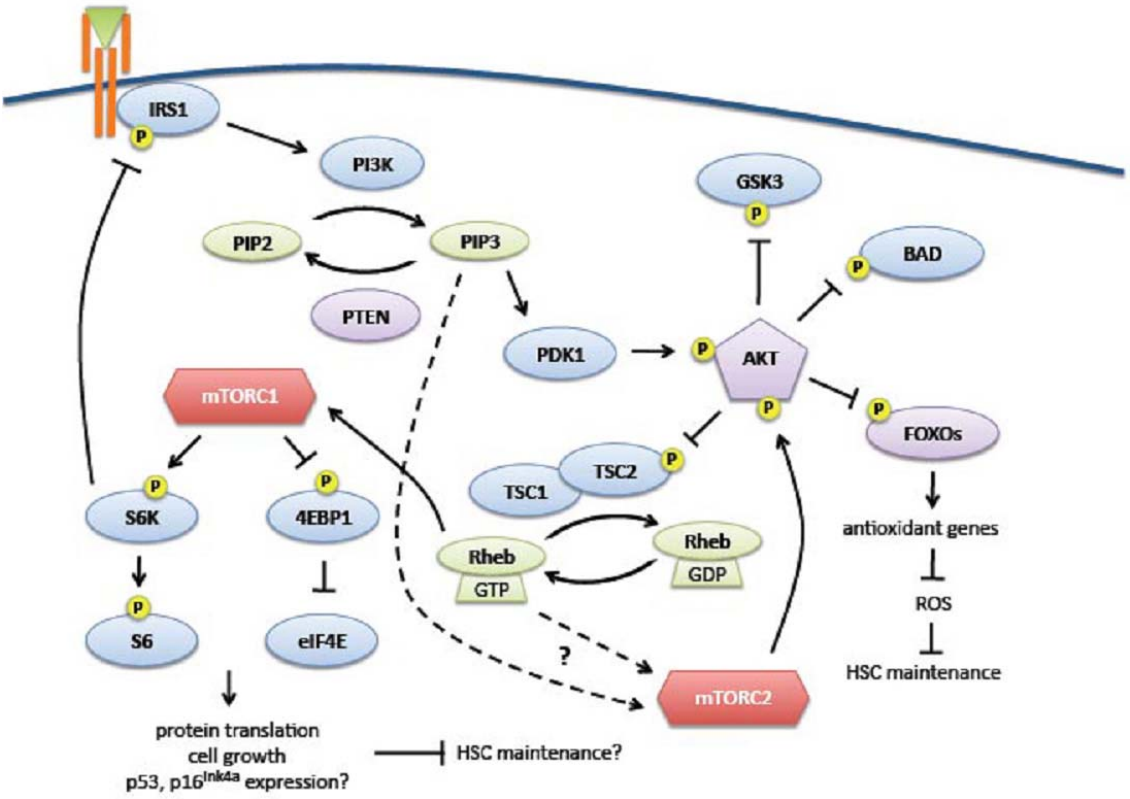

Figure S1: A schematic of PI-3kinase pathway signaling adapted from previously published reviews (Soulard and Hall, 2007; Laplante and Sabatini, 2009) (related to Fig. 1).

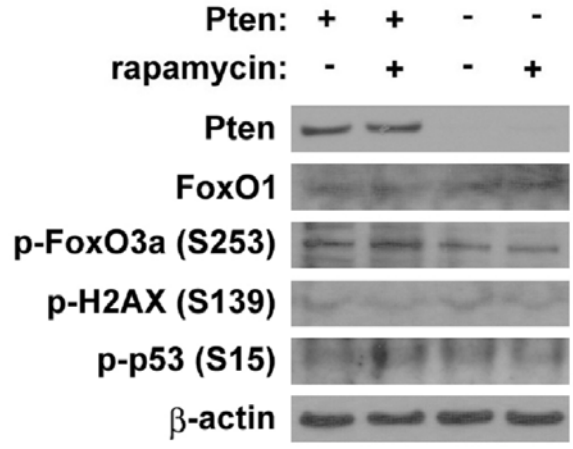

Figure S2: FoxO1, phospho-FoxO3a, and phospho-H2AX levels did not significantly change in hematopoietic stem/progenitor cells after *Pten* deletion (related to Figure 1). Control mice and *Pten*-deleted mice were treated with either vehicle or rapamycin for 1 week after pIpC treatment ended, then 200,000 $Lin^-c\text{-}kit^+Sca\text{-}1^+$ cells were sorted from each treatment and subjected to Western blotting. The levels of FoxO1 did not decrease and the levels of phospho-FoxO3a (S253) did not increase after *Pten* deletion. We were not able to detect FoxO4 expression in these cells (data not shown). The extent of DNA damage was estimated by blotting for phospho-H2AX (S139), which was detectable at very low levels in both control and *Pten*-deleted cells. We did not detect any change in phospho-p53 levels in $Lin^-c\text{-}kit^+Sca\text{-}1^+$ cells after *Pten* deletion. These blots are representative of 2 independent experiments.

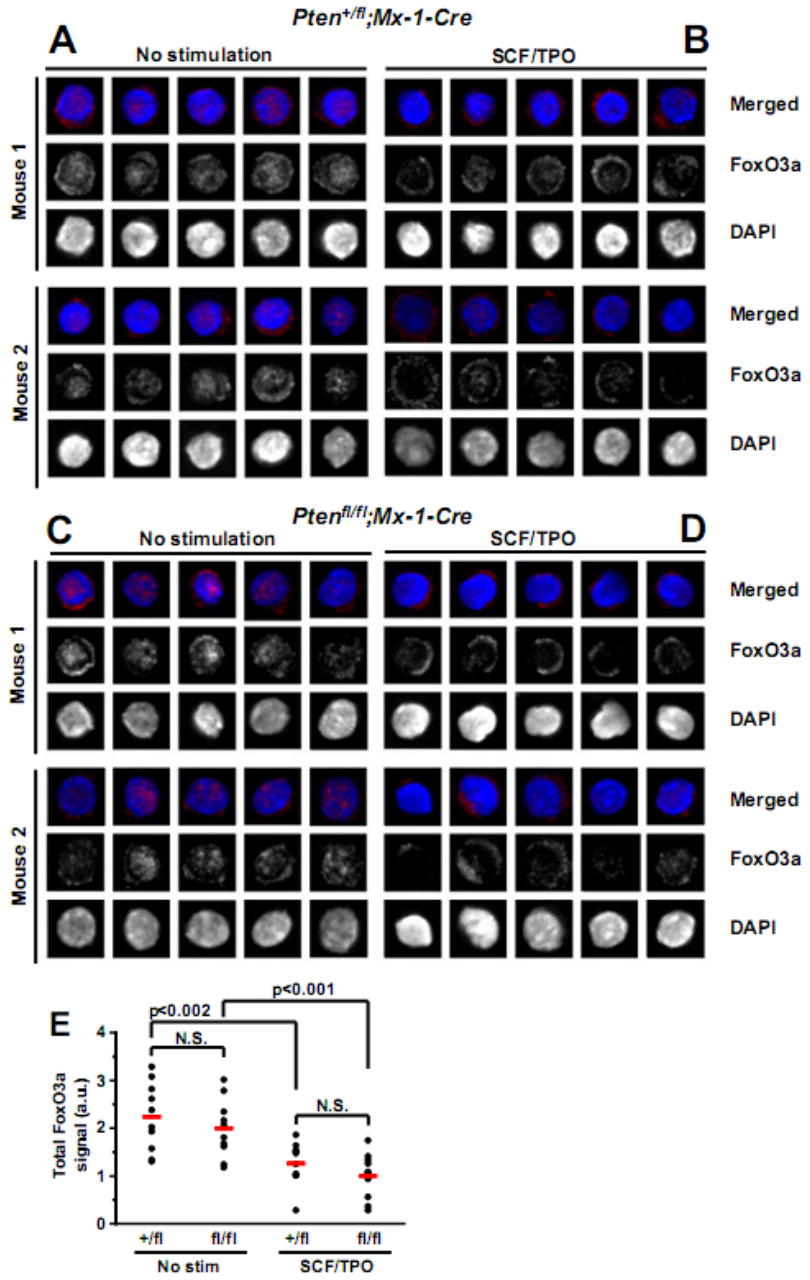

Figure S3: Stimulation of HSCs in culture with SCF and TPO reduced the levels of nuclear FoxO3a staining (related to Figure 1). $CD150^{+}CD48^{-}CD41^{-}Lin^{-}c\text{-}kit^{+}Sca\text{-}1^{+}$ HSCs from two control (A, B; *Pten*$^{+/fl}$*;Mx-1-Cre*$^{+}$) and two *Pten*-deficient (C, D; *Pten*$^{fl/fl}$*;Mx-1-Cre*$^{+}$) mice were incubated at 37°C in IMDM medium (+10% fetal bovine serum) with (B, D) or without (A, C) 20ng/ml SCF and 50ng/ml TPO. 24 hours later the cells were fixed, permeabilized, and stained for FoxO3a. Prominent nuclear FoxO3a staining was evident in both control (A) and *Pten*-deficient HSCs (C), similar to the staining observed in freshly isolated HSCs (Fig. 1F-G), but the total level of FoxO3a staining, and nuclear FoxO3a staining in particular, declined significantly ($p<0.002$ by Student's t-test; E) in HSCs of both genotypes that were stimulated with SCF and TPO (B, D). A total of 10 HSCs per treatment were imaged and quantified.

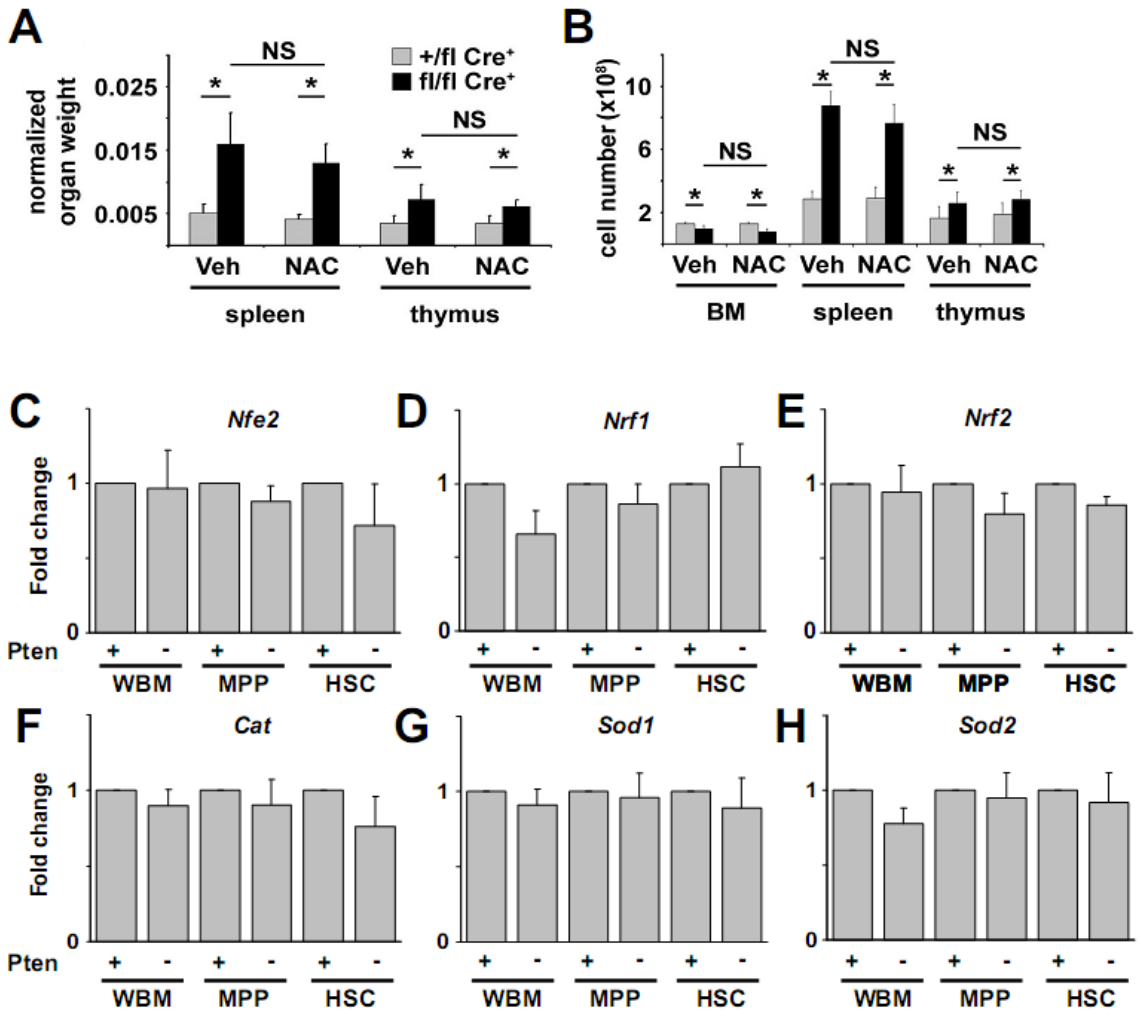

Figure S4: Treatment with N-Acetyl-cysteine (NAC) did not rescue the effects of *Pten* deletion on the cellularity of hematopoietic tissues and the expression levels of genes involved in the antioxidant response did not significantly change after *Pten* deletion (related to Figure 2). *Pten*$^{+/fl}$*;Mx-1-Cre*$^{+}$ and *Pten*$^{fl/fl}$*;Mx-1-Cre*$^{+}$ mice were injected with seven doses of pIpC over 14 days then daily subcutaneous injections of NAC or vehicle for 21 days. *Pten* deletion significantly (*, $p<0.005$ by Student's t-test) increased the mass (normalized to body mass; A) and cellularity (B) of the spleen and thymus but these changes were not affected by NAC treatment. Bone marrow cellularity significantly declined after *Pten* deletion but this change also was not affected by NAC (B). Data represent mean±standard deviation from 4 independent experiments with 1-2 mice/genotype/treatment. Expression levels of *Nfe2* (C), *Nrf1* (D), *Nrf2* (E), *catalase* (F), *Sod1* (G), and *Sod2* (H) were assessed by quantitative PCR in whole bone marrow (WBM) cells, CD150^{+}CD48^{-}CD41^{-}Lin^{-}c-kit^{+}Sca-1^{+} HSCs, and CD150^{-}CD48^{-}CD41^{-} Lin^{-}c-kit^{+}Sca-1^{+} MPPs harvested one week after pIpC treatment. The RNA content of samples was normalized based on *β-actin* and fold-change comparisons were made between *Pten*-deficient and control cells (control cells were set to 1 for purposes of the comparison). Data represent mean±SD from 2 independent experiments.

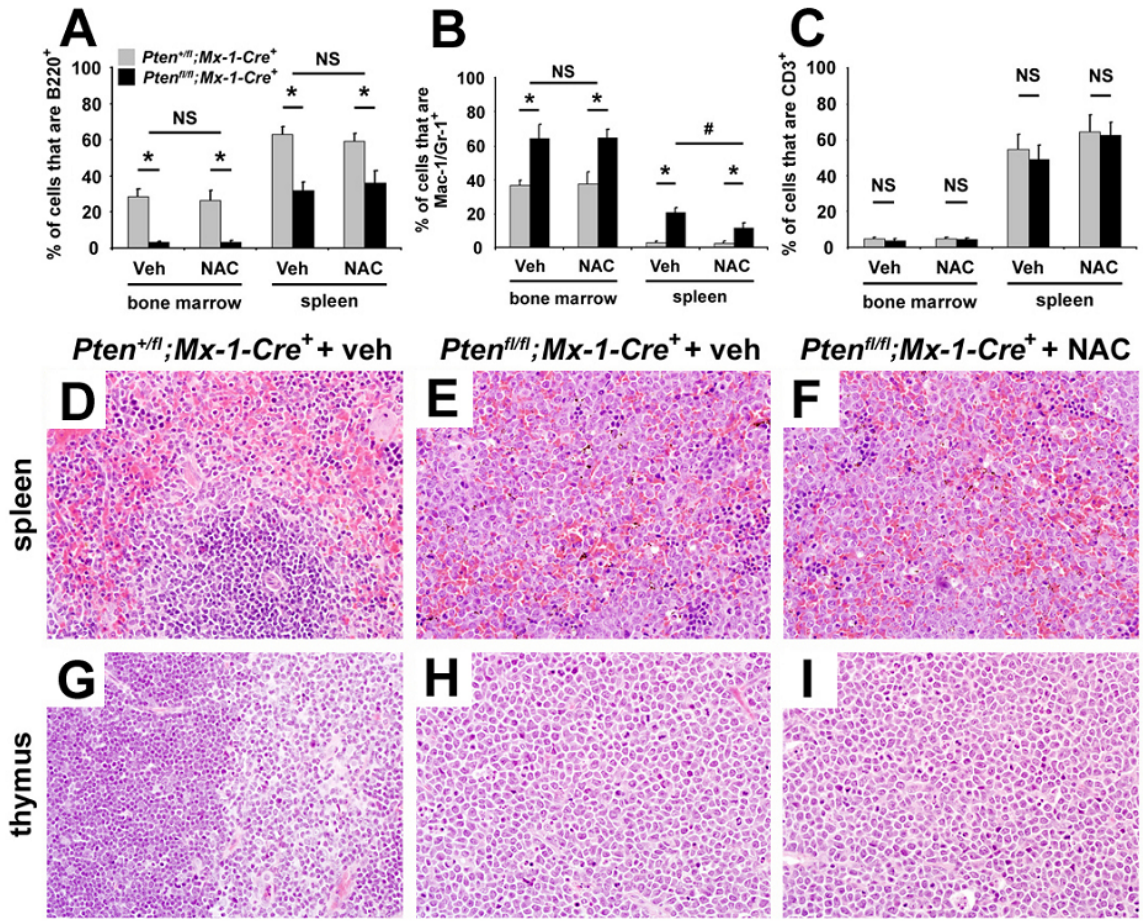

Figure S5: NAC treatment did not rescue the changes in hematopoiesis after *Pten* deletion nor did it prevent the development of T-ALL in recipients of *Pten*-deficient cells (related to Figure 3). NAC treatment did not affect the frequency of $B220^+$ B cells (A), $Mac\text{-}1^+Gr\text{-}1^+$ myeloid cells (B), or $CD3^+$ T cells (C) in the bone marrow or spleen of *Pten*-deleted (*Pten*$^{fl/fl}$;*Mx-1-Cre*$^+$) or control (*Pten*$^{+/fl}$;*Mx-1-Cre*$^+$) mice. (A) *Pten* deletion significantly (*, $p<0.0001$ by Student's t-test) reduced the frequency of $B220^+$ B cells in the bone marrow and spleen, but these decreases were not rescued by NAC treatment. All subpopulations of B-cells including $B220^+sIgM^-CD43^-$ pre-B cells, $B220^+sIgM^-CD43^{low}$ pro-B cells, and mature $B220^+sIgM^+$ cells were depleted by *Pten* deletion and were not rescued by NAC treatment (data not shown). (B) *Pten* deletion significantly increased the frequency of $Mac\text{-}1^+Gr\text{-}1^+$ myeloid cells in the bone marrow and spleen. NAC did not affect the increase in myeloid cells within the bone marrow but did attenuate the increase in the spleen (#, $p<0.001$ by Student's t-test). (C) Neither *Pten* deletion nor NAC treatment significantly affected the frequency of $CD3^+$ T cells in the bone marrow or spleen. All data represent mean±standard deviation from 4 independent experiments with 1-2 mice/genotype/treatment. The mice described in Figure 4F that had been transplanted with *Pten*-deficient or control bone marrow cells were examined for evidence of hematopoietic neoplasms. (D) Splenic architecture was normal in recipients of control bone marrow cells with clear boundaries between red and white pulp. (E) In recipients of *Pten*-deleted bone marrow cells the spleen was filled with lymphoid blasts and splenic architecture was completely effaced. (F) This was not affected by NAC treatment. (G) Thymic architecture was normal, with distinct cortex and medulla, in recipients of control cells. (H). In recipients of *Pten*-deleted bone marrow cells the thymus was filled with lymphoid blasts and thymic architecture was completely effaced. (I) This was not affected by NAC treatment.

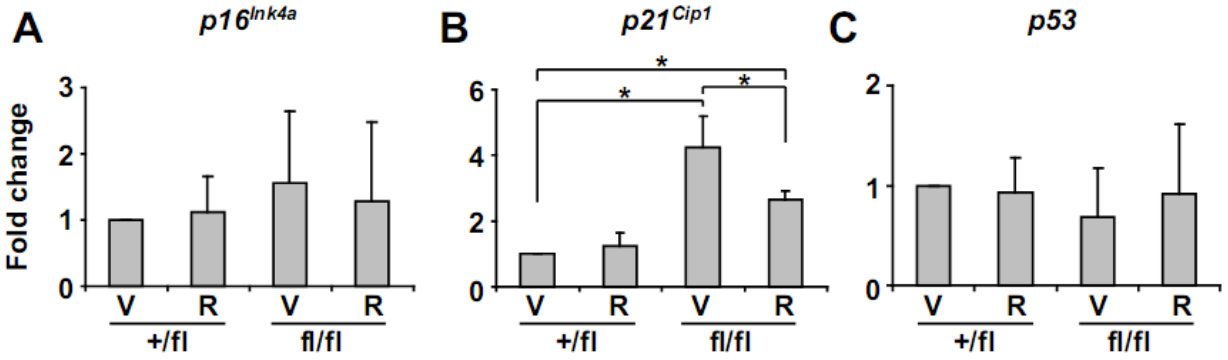

Figure S6: *Pten* deletion increased the levels of $p21^{Cip1}$ but not $p16^{Ink4a}$ or *p53* transcript in splenocytes (related to Figure 4). Splenocytes from mice described in Figure 5A were also tested for the induction of $p16^{Ink4a}$, $p21^{Cip1}$, and *p53* by quantitative (real-time) PCR. $p16^{Ink4a}$ and *p53* transcript levels were not significantly affected by *Pten* deletion or rapamycin treatment, but $p21^{Cip1}$ transcript levels were significantly (*, $p<0.05$ by Student's t-test) increased by *Pten* deletion and significantly reduced by rapamycin treatment. Data represent mean±standard deviation from 3 independent experiments.

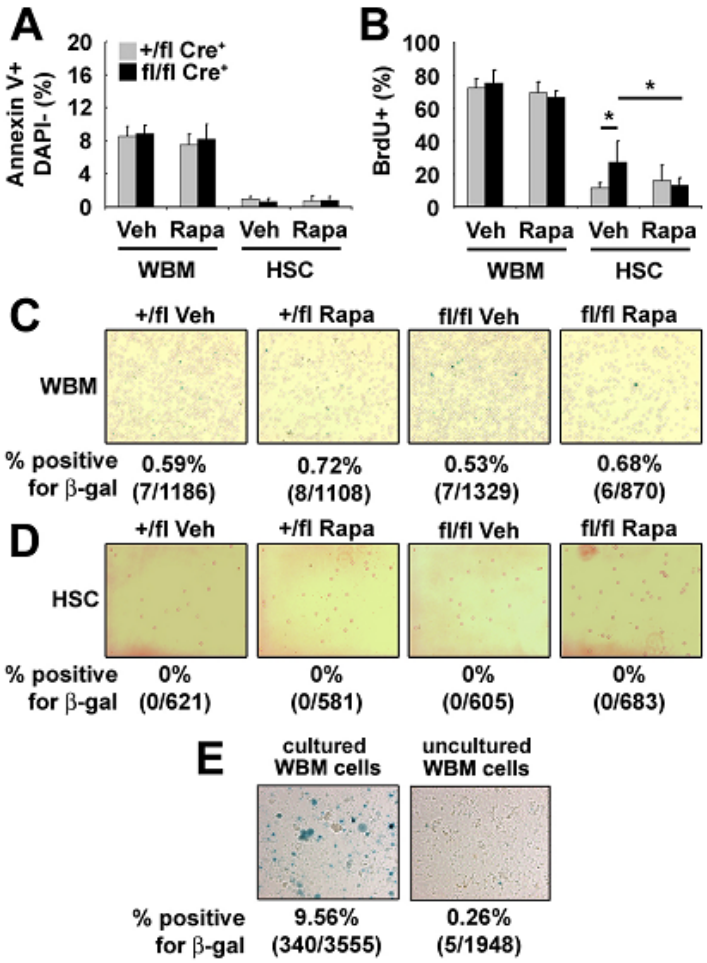

Figure S7: *Pten* deletion drove HSCs into cycle but did not detectably increase cell death or senescence in HSCs (related to Figure 6). (A) 3 weeks after *Pten* deletion, the frequency of whole bone marrow (WBM) cells or $CD150^{+}CD48^{-}CD41^{-}Lin^{-}c\text{-}kit^{+}Sca\text{-}1^{+}$ HSCs that were Annexin V^{+} $DAPI^{-}$ was not affected by *Pten* deletion or rapamycin treatment (mean±standard deviation from 3 independent experiments). (B) The rate of cell cycle entry was estimated by assessing the percentage of cells that incorporated BrdU over a 24 hour pulse administered 3 weeks after ending pIpC treatment. The frequency of $BrdU^{+}$ cells was significantly increased by *Pten* deletion and normalized by rapamycin treatment in HSCs but not significantly affected in WBM (*, $p<0.05$ by Student's t-test; data are mean±SD from 3 independent experiments). (C-E) Neither *Pten* deletion nor rapamycin treatment affected the frequency of ß-galactosidase expressing WBM cells (C; 870 to 1329 cells counted/treatment) or HSCs (D; 581 to 683 cells counted/treatment) obtained from mice 4 weeks after pIpC treatment ended. In each treatment, uncultured cells were sorted onto slides, then stained with X-gal, and counted. Rare X-gal stained cells (blue) were observed in WBM but not among HSCs. Culturing WBM cells increased the frequency of X-gal stained cells.

Table S1: Transplanting increasing numbers of $CD150^+CD48^-CD41^-Lin^-c\text{-}kit^+Sca\text{-}1^+$ cells from *Pten*-deleted mice with leukemia increased the percentage of recipient mice that developed leukemia (related to Figure 6).

10 $CD150^+CD48^-CD41^-Lin^-c\text{-}kit^+Sca\text{-}1^+$ cells transplanted			
Donor	**Total number of recipients**	**Recipients engrafted at 2 weeks**	**Recipients that developed leukemia**
A	35	22	7
B	14	10	5
C	10	4	1
D	10	3	1
50 $CD150^+CD48^-CD41^-Lin^-c\text{-}kit^+Sca\text{-}1^+$ cells transplanted			
Donor	**Total number of recipients**	**Recipients engrafted at 2 weeks**	**Recipients that developed leukemia**
E	15	10	10
F	20	18	18

SUPPLEMENTARY METHODS

Competitive repopulation and leukemogenesis assays: Wild-type adult recipient mice (CD45.1) were irradiated using a Cesium137 GammaCell40 Exactor Irradiator (MDS Nordia, Kanata, ON) delivering 110 rad/min in two equal doses of 570 rad, delivered at least 2 hr apart. Cells were injected into the retro-orbital venous sinus of anesthetized recipients. Each recipient mouse received 10 $CD150^{+}CD48^{-}CD41^{-}Lin^{-}Sca\text{-}1^{+}c\text{-}kit^{+}$ HSCs from CD45.2 donor mice (after pIpC treatment) along with 300,000 CD45.1 bone marrow cells for radioprotection. NAC treatment, when tested, started one day after transplantation. Beginning four weeks after transplantation and continuing for at least 16 weeks, blood from the tail veins of recipient mice, was subjected to ammonium-chloride potassium red cell lysis and stained with directly conjugated antibodies to CD45.2 (104), B220 (6B2), Mac-1 (M1/70), CD3(KT31.1), and Gr-1(8C5) to quantitate donor cell engraftment. For leukemogenesis assays, $1x10^{6}$ unexcised donor bone marrow cells were co-injected with 500,000 recipient bone marrow cells into irradiated wild-type recipient mice. Six weeks after transplantation, recipient mice were treated with seven injections of pIpC over 14 days and their survival was monitored over time. NAC treatment, when tested, was started after the final dose of pIpC.

Immunoprecipitation: Two million $Lineage^{-}c\text{-}kit^{+}$ progenitor cells were sorted and proteins were extracted by incubating on ice in lysis buffer (50 mM Tris-HCl, pH7.5, 150 mM NaCl, 1% Triton-X 100, 1mM EDTA) supplemented with complete EDTA-free protease inhibitor cocktail (Roche), 1mM PMSF and Halt phosphatase inhibitor cocktail (Pierce) with brief sonication. All extracts were precleared with Protein-L agarose (Santa Cruz Biotechnology) and incubated with Protein-L agarose and Protein A/G agarose bound with antibodies against p53 (#2524, Cell Signaling Technology), $p19^{Arf}$ (ab26696, Abcam) and $p16^{Ink4a}$ (sc-1207, Santa Cruz Biotechnology) or control IgG from mouse, rat, and rabbit for 12 hours at 4°C. Immunoprecipitates were washed four times with lysis buffer and heated to 70°C for 10 minutes in 1X LDS sample buffer (Invitrogen). The eluted proteins were separated on a Bis-Tris gel (Invitrogen) and immunoblotted with the antibodies indicated above. To detect p53, secondary antibodies against mouse IgG light chain (Jackson Immunoresearch) were used to prevent the IgG heavy chain from obscuring p53 detection.

Immunofluorescence assay: Immunofluorescence assays on sorted cells were performed as previously described (Ema et al., 2006). Cells were sorted into drops of PBS on poly-D-lysine coated slides and fixed with 2% paraformaldehyde for 10 minutes. In some experiments, cells were sorted into medium (IMDM + 10% fetal bovine serum) with or without SCF (20 ng/ml) and TPO (50 ng/ml), then incubated for 24 hours at 37°C and fixed. After washing, cells were permeabilized with PBS containing 0.3 % Triton X-100 and blocked with PBS containing 10% goat serum. Slides were stained with anti-FoxO3a (#2497) and anti-phospho-S6 (#2215) antibodies (Cell Signaling Technology, dilution 1:200) at 4°C overnight. After washing, slides were incubated with secondary antibodies conjugated with AlexaFluor 488 or 555 (Invitrogen) together with DAPI and analyzed with an FV-500 confocal microscope (Olympus).

Western blotting: The same number (25,000-50,000 depending on the experiment) of $c\text{-}kit^{+}Flk2^{-}Lin^{-}Sca\text{-}1^{+}CD48^{-}$ HSCs or whole bone marrow cells were sorted into microcentrifuge tubes with PBS and then protein was extracted by adding TCA to a final concentration of 10%. Extracts were incubated on ice for 15 minutes and spun down for 10 minutes at 16.1 rcf at 4°C. The supernatant was removed and the pellets were washed with acetone twice then dried. The protein pellets were solubilized with Solubilization buffer (9M Urea, 2% Triton X-100, 1% DTT) before adding LDS loading buffer (Invitrogen, Carlsbad, CA). For spleen and thymus samples, equivalent numbers of cells were pelleted, then lysed in RIPA buffer (50mM Tris, 150mM NaCl,

0.1% SDS, 0.5% Na deoxycholate, 1% Triton X-100) supplemented with complete EDTA-free protease inhibitors (Roche Applied Science, Indianapolis, IN), 1mM DTT, Halt phosphatase inhibitor cocktail (Thermo Fisher Scientific, Rockford, IL), and 1mM PMSF, spun down for 10 minutes at 16.1 rcf at 4°C. LDS loading buffer (Invitrogen) was added to the cleared supernatant. Proteins were separated on a Bis-Tris polyacrylamide gel (Invitrogen) and transferred to a PVDF membrane (Millipore, Billerica, MA). Antibodies used for Western blotting were anti-phospho Akt T308 (#4056), anti-Akt (#9272), anti-phospho-S6 (#2215), anti-S6 (#2217), anti-phospho-4E-BP1 (Thr37/46) (#2855), anti-4E-BP1 (#9452), anti-FoxO3a (#2497), and anti-p53 (#2524) (all from Cell Signaling Technology, Danvers, MA), and anti-$p16^{Ink4a}$ (sc-1207, Santa Cruz, Santa Cruz, CA), anti-$p19^{Arf}$ (ab26696, Abcam), anti-$p21^{Cip1}$ (sc-6246, Santa Cruz), and anti-ß-actin (A1978, Sigma).

Quantitative (real-time) reverse-transcriptase PCR: A total of 2000 HSCs or 20,000 unfractionated bone marrow cells were sorted into Trizol (Invitrogen) and RNA was isolated using chloroform extraction and isopropanol precipitation. cDNA was made with random primers and SuperScript III reverse transcriptase (Invitrogen). Quantitative PCR was performed with cDNA from 200 cell equivalents using a SYBR Green Kit and a LightCycler 480 (Roche Applied Science). Each sample was normalized to β-actin. Primer sequences were as follow: β-actin F, 5'- CGTCGACAACGGCTCCGGCATG and β-actin R, 5'- GGGCCTCGTCACCCACATAGGAG; Nfe2 F, TGGCCATGAAGATTCCTTTC and Nfe2 R, TAGCGGATACTGTGCCAACA; Nrf1 F, GTCACCATGGCCCTCAAC and Nrf1 R, GGACTATCTGTCTCCCACCTTG; Nrf2 F, CATGATGGACTTGGAGTTGC and Nrf2 R, CCTCCAAAGGATGTCAATCAA; catalase F, CCTTCAAGTTGGTTAATGCAGA and catalase R, CAAGTTTTTGATGCCCTGGT; SOD1 F, GTGACTGCTGGAAAGAACG and SOD1 R, TCTCGTGGACCACCATTGTA; SOD2 F, GGCTTGGCTTCAATAAGGAG and SOD2 R, ATACTGAAGGTAGTAAGCGTG; Ink4a F, CGAACTCTTTCGGTCGTACCC and Ink4a R, CGAATCTGCACCGTAGTTGAGC; Arf F, GTTCTTGGTCACTGTGAGGATTCAG and Arf R, CCATCATCATCACCTGGTCCAG; Cip1 F, TCCACAGCGATATCCAGACA and Cip1 R, AGACAACGGCACACTTTGCT; Trp53 F, AAAGGATGCCCATGCTACAG and Trp53 R, TATGGCGGGAAGTAGACTGG.

Annexin V, BrdU, and senescence-associated β-galactosidase staining: Annexin V was detected by flow-cytometry using Annexin V APC (BD PharMingen) and Annexin V Binding Buffer (BD PharMingen) as described by the manufacturer. BrdU incorporation was measured by flow-cytometry (BD PharMingen). As described previously (Cheshier et al., 1999), mice were given an intraperitoneal injection of 0.1 mg of BrdU/g of body mass in Dulbecco's phosphate buffered saline (D-PBS, Gibco). For senescence-associated β-galactosidase staining, cells were sorted into drops of PBS on a poly-lysine coated slide and stained using the senescence-associated β-gal Staining Kit (#9860, Cell Signaling Technology).

Histopathology: Spleen, liver, and thymus samples were fixed in 10% neutral buffered formalin and paraffin embedded. Thin sections (5 µm) were cut on a microtome and stained with hematoxylin and eosin using standard protocols. The slides were then analyzed with a hematopathologist and classified according to the Bethesda protocols for the classification of hematopoietic neoplasms in mice (Kogan et al., 2002; Morse et al., 2002).

SUPPLEMENTARY REFERENCES

Cheshier, S., Morrison, S.J., Liao, X., and Weissman, I.L. (1999). In vivo proliferation and cell cycle kinetics of long-term self-renewing hematopoietic stem cells. Proceedings of the National Academy of Sciences USA *96*, 3120-3125.

Ema, H., Morita, Y., Yamazaki, S., Matsubara, A., Seita, J., Tadokoro, Y., Kondo, H., Takano, H., and Nakauchi, H. (2006). Adult mouse hematopoietic stem cells: purification and single-cell assays. Nat Protoc *1*, 2979-2987.

Kogan, S.C., Ward, J.M., Anver, M.R., Berman, J.J., Brayton, C., Cardiff, R.D., Carter, J.S., deCoronado, S., Downing, J.R., Fredrickson, T.N.*, et al.* (2002). Bethesda proposals for classification of nonlymphoid hematopoietic neoplasms in mice. Blood *100*, 238-245.

Laplante, M., and Sabatini, D.M. (2009). mTOR signaling at a glance. Journal of cell science *122*, 3589-3594.

Morse, H.C., Anver, M.R., Fredrickson, T.N., Haines, D.C., Harris, A.W., Harris, N.L., Jaffe, E.S., Kogan, S.C., MacLennan, I.C.M., Pattengale, P.K.*, et al.* (2002). Bethesda proposals for classification of lymphoid neoplasms in mice. Blood *100*, 246-258.

Soulard, A., and Hall, M.N. (2007). SnapShot: mTOR signaling. Cell *129*, 434.